Power Switching Based on Trajectory Planning and Sliding Mode Control for Solid Oxide Fuel Cell Systems

Zhen Wang, Guoqiang Liu, Xingbo Liu, Jie Wang, Zhiyang Jin, Xiaowei Fu, Zhuo Wang, Bing Jin, Zhonghua Deng, and Xi Li

***Abstract*—To improve the safety of the solid oxide fuel cell (SOFC) systems and avoid the generation of large amounts of pollutants during power switching, this paper designs a power switching strategy based on trajectory planning and sliding mode control (TP-SMC). The design elements of the power switching strategy are proposed through simulation analysis at first. Then, based on the gas transmission delay time and the change of gas flow obtained from testing, trajectory planning (TP) is implemented. Compared with other power switching strategies, it has been proven that the power switching strategy based on TP has significantly better control performance. Furthermore, considering the shortcomings and problems of TP in practical application, this paper introduces sliding mode control (SMC) on the basis of TP to improve the power switching strategy. The final simulation results also prove that the TP-SMC can effectively suppress the impact of uncertainty in gas flow and gas transmission delay time. Compared with TP, TP-SMC can ensure that under uncertain conditions, the SOFC system does not experience fuel starvation and temperature exceeding limit during power switching. Meanwhile, the NOx emissions are also within the normal and acceptable range. This paper can guide the power switching process of the actual SOFC systems to avoid safety issues and excessive generation of NOx, which is very helpful for improving the performance and service life of the SOFC systems.**

***Index Terms*—Solid oxide fuel cell (SOFC) system, power switching, safety, NOx emission, trajectory planning, sliding mode control.**

I. Introduction

SOLID oxide fuel cell (SOFC), as a new power generation technology, has attracted widespread attention over the world [1], [2]. Compared with the conventional power production technologies, the SOFC systems can directly convert chemical energy into electrical energy, with higher efficiency, lower pollutant emissions, and less noise [3] - [5]. Therefore, SOFC systems have enormous development potential and are now applied in various fields such as fixed power station, combined heat and power (CHP) system, and vehicle power supply [6]-[8].

The application challenges of the SOFC systems mainly focus on three aspects: efficiency, safety, and service life [9]-[12]. How to ensure the safety, efficiency, and long-term operation of the SOFC systems is the goal pursued by all researchers. Among these three application challenges, safety is the foundation, efficiency is the goal, and service life is the pursuit.

In the past decade, many scholars have studied the three application challenges of the SOFC systems. Temperature safety is crucial for the normal operation of the SOFC systems. Besides, ensuring the highest system efficiency within the safe temperature range is an important issue. In order to maximize the efficiency of the SOFC systems within a safe temperature range, [13] conducts steady-state analysis and optimization of the SOFC systems, and concludes that the optimal operation points (OOPs) can be determined by maximizing the system efficiency while enforcing the operation constraints on the maximum positive-electrolyte-negative (PEN) temperature and its gradient. Reference [14] takes an analysis on optimization of a kilowatt-scale SOFC standalone system for the maximum system efficiency and considers four temperature constraints. Reference [15] proposes an analysis-based optimization method for discrete optimization with constraints to obtain the optimal operation point with

Manuscript received: March 16, 2024; revised: May 10, 2024; accepted: May 28, 2024. Date of CrossCheck: May 28, 2024. Date of online publication: November 7, 2024.

This work was supported by the National Key Research and Development Program of China (No. 2022YFB4003805), Jiangsu Key Research and Development Program (No. BE2023092-3), Hubei Province Local Leaded by Central Science and Technology Development Special Project (No. 2023EG001), and International Science and Technology Cooperation Project in Hubei Province (No. 2022EHB011).

Z. Wang, G. Liu, J. Wang, Z. Jin, Z. Wang, and X. Li (corresponding author) are with the Key Laboratory of Imaging Processing and Intelligent Control of Ministry of Education, School of Artificial Intelligence and Automation, Huazhong University of Science and Technology, Wuhan, China, and X. Li is also with the Research Institute of Huazhong University of Science and Technology in Shenzhen, Shenzhen, China (e-mail: 1480725206@qq.com; liuguoqiang@hust.edu.cn; 1540226827@qq.com; u202111415@hust.edu.cn; wangzhuo@hust.edu.cn; lixi_ wh@126.com).

X. Liu and B. Jin are with the Hubei Huazhong Electric Power Technology Development Co., Ltd., Wuhan, China (e-mail: lxb0829@qq.com; iceking0921@qq.com).

X. Fu is with the School of Computer Science and Technology, Wuhan University of Science and Technology, Wuhan, China (e-mail: fxw_wh0409@wust.edu.cn).

Z. Deng is with the School of Artificial Intelligence and Automation, Huazhong University of Science and Technology, Wuhan, China, and he is also with the Wuhan Huamao Automation Co., Ltd., Wuhan, China (e-mail: zhonghua.deng@mail.hust.edu.cn).

DOI: 10.35833/MPCE.2024.000284

the maximum efficiency and temperature safety. Reference [16] proposes an optimal robust control strategy to maintain the safe operation of the SOFC systems with the maximum efficiency. Reference [17] conducts a detailed parameter study on the cross-flow configuration to optimize cell performance and system efficiency by minimizing thermal stress. Although the above literature has studied the security and efficiency issues of the SOFC systems, these studies are all focused on steady-state operation processes, few of which have paid attention to safety issues during power switching.

Generally, the SOFC systems can obtain a series of OOPs through steady-state analysis. The emergence of the OOPs can ensure that the SOFC systems are in a safe and efficient state during normal steady-state operation. Although the SOFC systems generally operate in a steady state, the change of external load also requires power conversion by the SOFC system, and safety is the primary consideration at this time. During the power switching process, the SOFC systems mainly encounter two safety issues: fuel starvation and temperature exceeding. References [18] and [19] determine the OOPs for various steady-state output power with the goal of the maximum efficiency. Then, the issues of fast load and safe transient operation during load step-up transitions are studied. However, these research works only investigate whether fuel starvation occurs at different linear switching rates under different assumed transmission delays. Moreover, they do not explain the basis for choosing a parabola as the current variation curve, but only make relevant comparisons. Reference [20] develops a novel thermoelectric collaborative controller that can simultaneously achieve fast power tracking, system thermal management, and system efficiency optimization. However, this research work only controls the temperature through the feedback control of gas flow, and the fuel starvation problem is similar to [19]. Reference [21] focues on the issue of fuel starvation and develops various methods to prevent fuel starvation in fuel cells. However, this research work only considers the issue of fuel starvation during power switching, without considering temperature issues at all. Meanwhile, the impact of gas transmission delay is not considered. References [22]-[25] have conducted research on the power switching process of the SOFC systems, but they only focus on the fast tracking of power, with little attention paid to the fuel starvation and temperature exceeding issues during the switching process. Although many scholars have studied the power switching process of the SOFC systems, some scholars only focus on fast power tracking without considering safety issues. Some scholars only consider fuel starvation issues without considering temperature safety issues. Even though some scholars have considered various safety issues, they have not truly considered the changes in gas flow and gas concentration in the stack when designing power switching strategies, and there is no real design basis for the current change process. In addition, although the pollutant emissions of the SOFC system are very small, the change of gas concentration and temperature may cause a sudden increase in pollutant emissions during the power switching process, which must also be noted and controlled in the SOFC system.

The aim of this study is to design a power switching strategy to avoid fuel starvation and temperature exceedance during the power switching process. Besides, the issue of pollutant emissions during power switching has also been considered. Firstly, through simulation analysis, the design elements of the power switching strategy are proposed. Then, based on the delay time of gas transmission and the change of gas flow obtained from testing, the trajectory planning (TP) is implemented. Furthermore, considering the shortcomings and problems of TP in practical application, this paper introduces the sliding mode control (SMC) on the basis of TP.

The remainder of this paper is organized as follows. Section II establishes the SOFC system model and NOx formation model. Section III presents the problem description and solution direction during power switching in SOFC system. Section IV presents the power switching strategy based on TP. Section V introduces the improved power switching strategy with SMC. Finally, Section VI concludes the paper.

II. SOFC System Model and NOx Formation Model

A. SOFC System Model

The SOFC stack must be equipped with corresponding balance of plant (BOP) to form a complete independent power generation system. The traditional pure hydrogen SOFC system mainly consists of five subsystems: fuel supply pipeline and valves, air supply pipeline and valves, SOFC stack, exhaust gas recovery subsystem (including burner and heat exchanger), and electronic control subsystem. Figure 1 shows the schematic diagram of SOFC system, where HEX is short for heat exchanger.

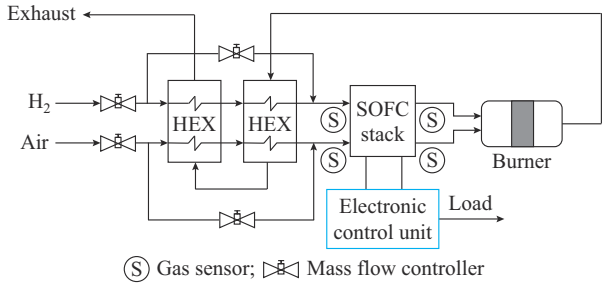

Fig. 1. Schematic diagram of SOFC system.

The SOFC stack is the core device of the SOFC system, and its model can be divided into three parts: electrochemical model, mass conservation model, and energy conservation model. The BOP mainly includes blower, heat exchangers, and burner and gas supply subsystem. They are integrated with the fuel stack to form the entire system model.

Several dynamic models can be found and validated by our groups in literature for the SOFC systems, including those developed by [18], [26], and [27], as well as those by other groups [28]-[32].

In order to simplify the model, several assumptions are made during the solution process in each control volume. The common assumptions are as follows:

1) All gases are ideal gases.

2) Variables in control volumes such as the current density, temperatures, and pressures are assumed to be homoge-

neous.

3) There is no heat transfer to the environment. The system is assumed to be well insulated.

4) There is no carbon formation or deposition.

5) Each cell is considered to operate identically.

B. NOx Formation Model

Due to the high-temperature environment of the burner, NO will be produced. NO from combustion systems is generated by three main processes: thermal-NO, prompt-NO, and fuel-NO [33], [34]. Due to the fact that the fuel used by the burner in the SOFC system is gaseous and the burner is a fuel-lean environment, the burner mainly produces thermal-NO. The thermal-NO mechanism originally proposed by [34]-[36] includes two reactions:

$$\mathrm{N_2+O=NO+N} \tag{1}$$

$$\mathrm{O_2+N=NO+O} \tag{2}$$

Usually, the follow reaction is also considered in the thermal-NO formation.

$$\mathrm{N+OH=NO+H} \tag{3}$$

The general rate equation for NO generated by these three processes is:

$$\frac{\mathrm{d[NO]}}{\mathrm{d}t}=2[\mathrm{O}]\frac{(k_1[\mathrm{N_2}]-k_{-1}k_{-2}[\mathrm{NO}]^2/k_2[\mathrm{O_2}])}{1+k_{-1}[\mathrm{NO}]/(k_2[\mathrm{O_2}]+k_3[\mathrm{OH}])} \tag{4}$$

where [·] denotes the concentration; k_i, $i\in\{1,2,3\}$ and k_{-j} $j\in\{1,2\}$ are the forward reaction rate constant and reverse reaction rate constant, respectively.

If the concentration of NO is very small, the rate of NO formation can be approximated as [35], [37]:

$$\frac{\mathrm{d[NO]}}{\mathrm{d}t}=2k_1[\mathrm{O}][\mathrm{N_2}] \tag{5}$$

where $k_1=1.8\times10^{14}\mathrm{e}^{-38300/T_B}$, and T_B is the temperature of burner.

To model the NO formation, it is necessary to estimate the concentration of O-atoms [O]. Here are two models to estimate [O].

1) Model 1: the first model assumes partial equilibrium of the reaction [38], [39]:

$$\frac{1}{2}\mathrm{O_2=O} \tag{6}$$

The concentration of O-atoms can be written as [38]:

$$[\mathrm{O}]=\frac{3600\mathrm{e}^{-61750/RT_B}}{\sqrt{RT_B}}[\mathrm{O_2}]^{0.5} \tag{7}$$

where R is the universal gas constant.

2) Model 2: this model is based on the assumption of partial equilibrium of the chain-branching and propagation reactions of the hydrogen-oxygen mechanism [35], [39]:

$$\mathrm{O+H_2=OH+H} \tag{8}$$

$$\mathrm{H+O_2=OH+O} \tag{9}$$

$$\mathrm{OH+H_2=H_2O+H} \tag{10}$$

We can estimate [O] as:

$$[\mathrm{O}]=\frac{k_9k_{10}}{k_{-9}k_{-10}}\frac{[\mathrm{O_2}][\mathrm{H_2}]}{[\mathrm{H_2O}]} \tag{11}$$

where $k_9=1\times10^{14}\mathrm{e}^{-7470/T_B}$; $k_{-9}=1.4\times10^{13}\mathrm{e}^{-353/T_B}$; $k_{10}=1\times10^8T^{1.6}\mathrm{e}^{-1660/T_B}$; and $k_{-10}=4.5\times10^8T_B{}^{1.6}\mathrm{e}^{-9270/T_B}$ [36], [38].

Compared with Model 1, Model 2 is more comprehensive and takes into account the impact of hydrogen gas. However, when there is fuel starvation in the SOFC system ($[\mathrm{H_2}]=0$), there may be problems in the calculation. Therefore, this paper comprehensively considers these two scenarios: Model 1 is used when the $\mathrm{H_2}$ concentration at the stack outlet is less than 5%, and Model 2 is used when it is greater than 5%. The final NOx formation model is:

$$\frac{\mathrm{d[NO]}}{\mathrm{d}t}=\begin{cases}\dfrac{2k_1k_9k_{10}[\mathrm{H_2}][\mathrm{O_2}][\mathrm{N_2}]}{k_{-9}k_{-10}[\mathrm{H_2O}]} & \varphi_{H_2,out}\geq5\% \\ 2k_1\dfrac{3600\mathrm{e}^{-61750/RT_B}}{\sqrt{RT_B}}[\mathrm{O_2}]^{0.5}[\mathrm{N_2}] & \varphi_{H_2,out}<5\%\end{cases} \tag{12}$$

where $\varphi_{H_2,out}$ is the $\mathrm{H_2}$ concentration at the stack outlet.

III. Problem Description and Solution Direction During Power Switching in SOFC System

A. Gas Flow Test

To determine the change process of actual gas flow, this paper tests the change of actual gas flow by changing the gas flow setting value in steps. The test scheme for the change of gas flow is shown in Table I, where SLM represents the standard litre per min. Finally, two groups are actually tested, and all gas flow values have been normalized to ensure that the gas flow values are within the range [0,1].

TABLE I
Test Scheme for Change of Gas Flow

Initial flow (SLM)	Final flow (SLM)	Switching process	Test group
15	12	15→12	Test 1, test 4
15	10	15→10	Test 2, test 5
15	8	15→8	Test 3, test 6

For the change of gas flow, it can be observed as an inertial element. Therefore, the flow controller model can be written as $1/(Ts+1)$ in the simulation. The comparison of the change of gas flow with actual test data under different time constants T is shown in Fig. 2.

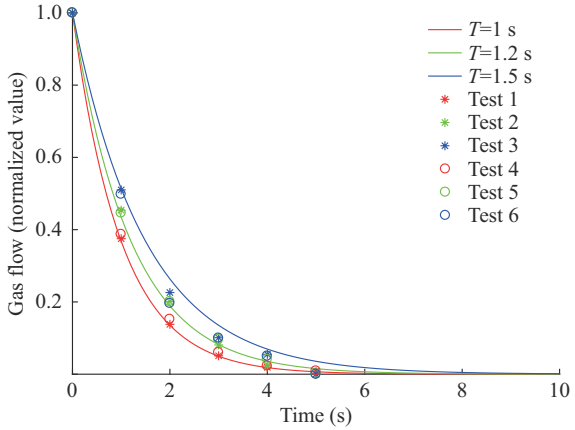

Fig. 2. Comparison of change of gas flow with actual test data.

Figure 2 shows that the actual test data are close to the inertial response curve with $T=1.2$ s, and all data are within the range of the inertial response curves with $T=1$ s and $T=1.5$ s.

B. Problems in Power Switching Process

1) Switching from Low Power to High Power

In order to study the dynamic characteristics of power switching in the SOFC system, the SOFC system switches from half load (500 W) to full load (1 kW) at 30000 s, with a step increase in output power. The corresponding OOPs, namely *I*, *BP*, *AR*, *FU*, are 20, 0.05, 6, 0.9 and 48, 0, 6, 0.85, respectively.

Under the above switching conditions, the gas flow is an inertial change with $T=1.2$ s. At the same time, the current changes linearly from 30000 s. The fuel margin (i.e., hydrogen concentration) and burner temperature T_{burner} of the SOFC system from half load to full load under different current switching rates are shown in Fig. 3.

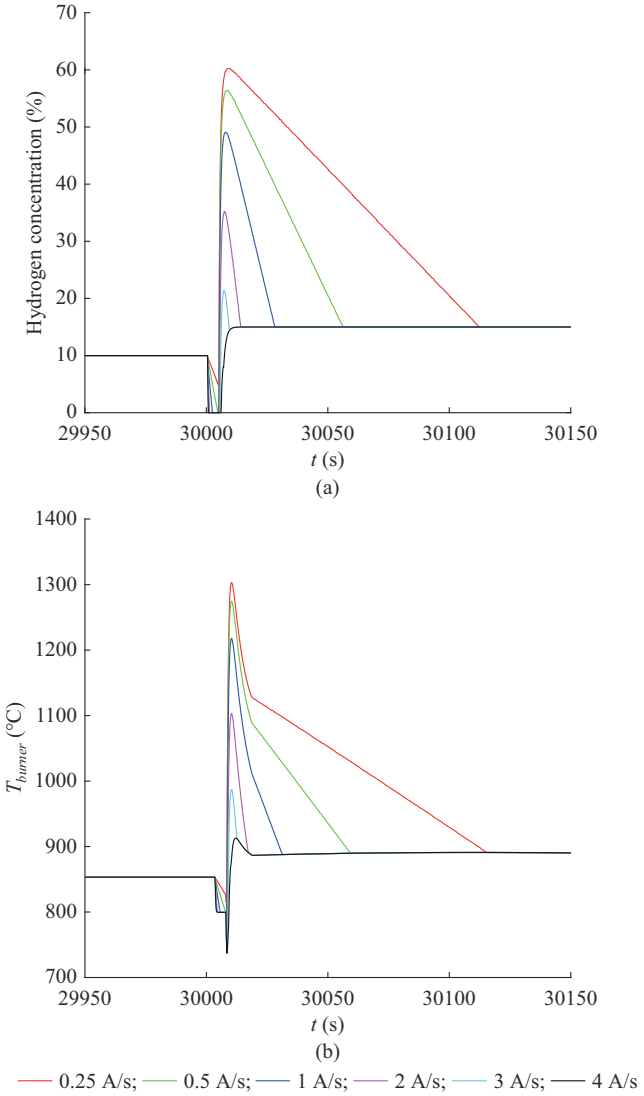

Fig. 3. Fuel margin and burner temperature of SOFC system from half load to full load. (a) Hydrogen concentration. (b) T_{burner}.

Figure 3 shows that if the hydrogen concentration is too high, the fuel starvation will occur. This is because there is a delay in gas transmission within the SOFC system when switching from low power to high power. If the current switching rate is too high, fuel starvation will occur due to excessive current during the period of gas transmission delay. To avoid fuel starvation, the current switching rate should not exceed 0.5 A/s. However, if the current switching rate is too low, the burner temperature will exceed the upper temperature limit (1000 °C). This is because a small current can cause an excessive fuel margin at the stack outlet. These fuels will generate a large amount of heat during combustion in the burner, causing the burner temperature to exceed the limit. In order to avoid exceeding the burner temperature limit, the current switching rate should not be less than 3 A/s. Obviously, these two are contradictory to each other. Under the present switching strategy, there will inevitably be a security constraint condition that is not met.

2) Switching from High Power to Low Power

The SOFC system switches from full load (1 kW) to half load (500 W) at 30000 s, with a step decrease in output power. The fuel margin and burner temperature of the SOFC system under different current switching rates are shown in Fig. 4.

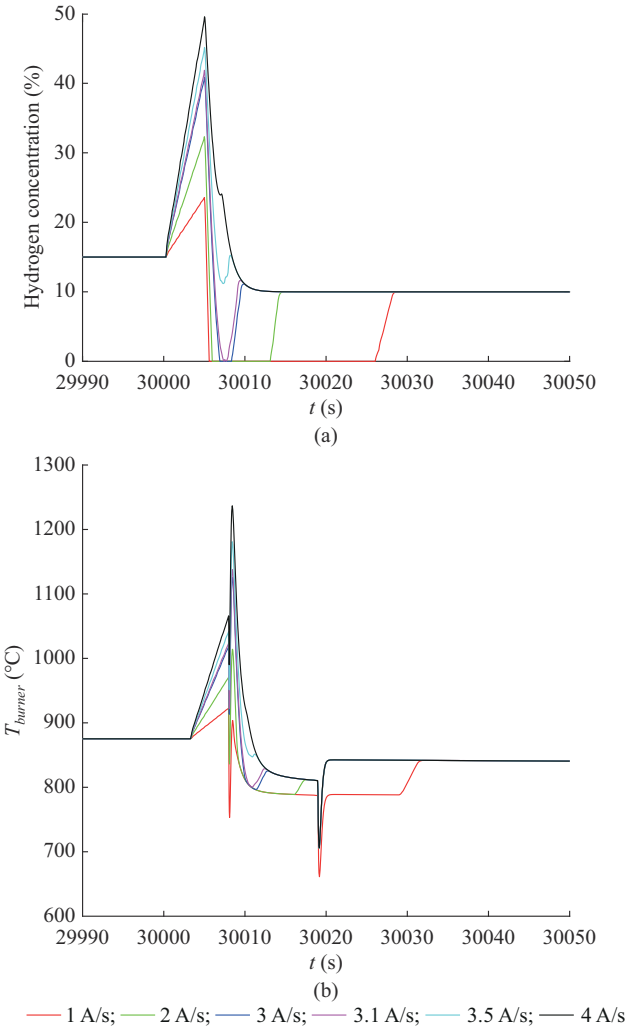

Fig. 4. Fuel margin and burner temperature of SOFC system from full load to half load. (a) Hydrogen concentration. (b) T_{burner}.

Figure 4 shows that if the current switching rate is too low, the fuel starvation will occur. This is because when the gas flow under the new operation conditions is transmitted to the stack after a time period, the gas flow inside the stack decreases. If the current switching rate is too low and causes the current to be too large, the fuel starvation will occur. To avoid fuel starvation, the current switching rate should not be less than 3.1 A/s. However, if the current switching rate is too high, the burner temperature will exceed the upper temperature limit (999.85 ℃). This is because during the period of gas transmission delay, the gas flow inside the SOFC stack is still under full power conditions. If the current switching is too fast and the stack current I_{cell} is too small, it will cause excessive fuel to enter the burner, leading to the burner temperature exceeding the limit. To avoid exceeding the burner temperature limit, the current switching rate should not exceed 2 A/s. Similarly, these two are also contradictory to each other.

C. Impact of Power Switching on NOx Emissions

During the power switching process, the SOFC system may experience fuel starvation and temperature exceeding limit, which will inevitably affect the NOx emissions in the burner. Based on the above research, the NOx emissions in the burner under different conditions are studied, and the results are shown in Fig. 5.

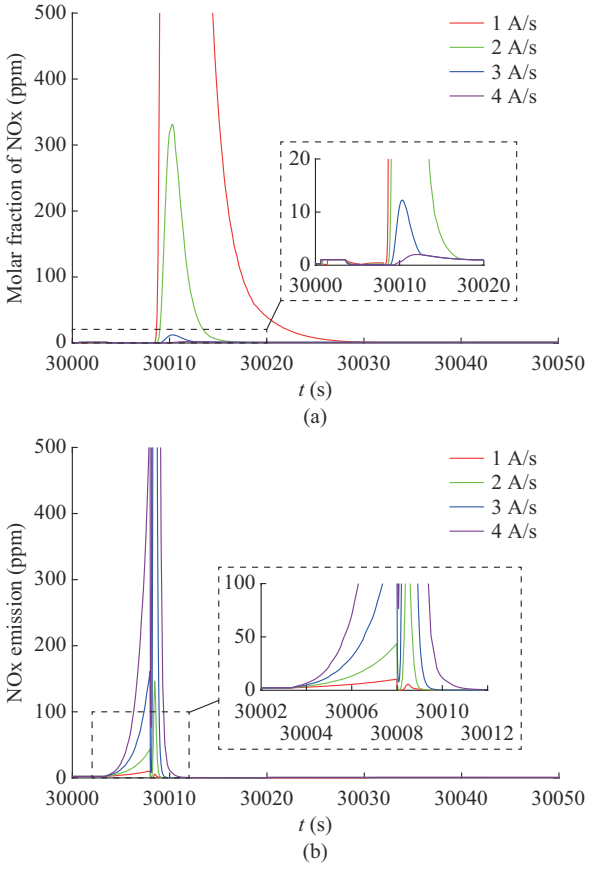

Fig. 5. NOx emission characteristics of burner. (a) Molar fraction of NOx from half load to full load. (b) NOx emission from full load to half load.

Figure 5 shows that when the SOFC system operates normally and stably, the NOx formation in the burner is below 10 ppm. Note that ppm represents parts per million of volume concentration. However, during power switching process, the NOx emissions from the burner will increase due to the change of gas concentration and burner temperature. Meanwhile, compared with Fig. 3 and Fig. 4, it can be observed that the main factor affecting NOx emissions is temperature. As the temperature increases, the NOx emissions from the burner will also sharply increase. Therefore, in order to reduce NOx emissions, it is also necessary to control the burner temperature during the power switching process.

D. Design Elements of Power Switching Strategy

From the above analysis, it can be concluded that the problems of fuel starvation and temperature exceeding limit during the power switching process of the SOFC system can be summarized as numerical problems. When the current is too large at a certain moment, it will cause fuel starvation, while when the current is too small at a certain moment, the burner temperature will exceed the limit. It is worth noting that the excessive and insufficient current mentioned above is relative to the present gas flow of the SOFC stack. In addition, the NOx emissions of the SOFC system are also related to the burner temperature. If the problem of temperature exceeding limit during power switching can be solved, the NOx emission problem in the SOFC system will also be solved accordingly. Therefore, the core of the power switching process is to ensure that the current is within a reasonable range during the power switching process.

There are two factors that affect the current value during the power switching process. One is the current switching point (the time point at which the current begins to change), and the other is the law of current variation. For the selection of current switching points, it is necessary to ensure that both the current and gas flow inside the SOFC stack change simultaneously. For the law of current variation, it is necessary to ensure that the fuel margin and temperature characteristics of the SOFC system are under best values.

IV. Power Switching Strategy Based on TP

In this section, the gas transmission delay time is first determined through test, and then the corresponding power switching strategy is designed. Finally, the superiority of the power switching strategy designed in this paper is verified through comparison.

A. Gas Transmission Test

To determine the gas transmission delay time, we stabilize the stack current, change the input gas flow, and detect the change of gas concentration at the stack outlet. Obviously, the time from changing the gas flow to discovering a change in gas concentration is the gas transfer time from the flow controller to the stack outlet. Finally, the gas transmission delay time from the flow controller to the stack inlet can be determined by testing the gas transmission delay time inside the SOFC stack using the corresponding stack test bench.

We define the gas transfer time from the flow controller to the stack inlet as the current switching delay time t_d and

the gas transfer time inside the SOFC stack as the stack transfer time t_s. Through test, the gas transfer time from the flow controller to the stack outlet is approximately 6 s. Assume a gas transfer time of 1 s within the stack. Therefore, in this paper, $t_d = 5$ s and $t_s = 1$ s.

B. Design and Performance Verification of Power Switching Strategy

When the change law of gas flow and the gas transmission delay time are known, the trajectory of current variation in the SOFC stack can be planned. This power switching strategy is called TP. In order to verify the superiority of the power switching strategy designed in this paper, it will be compared with other power switching strategies. The switching strategies used for comparison are linearity switching, step switching, and multistep switching. Four different switching strategies are shown in Fig. 6.

Through simulation research, the performances of four different power switching strategies are compared. In the simulation, the change of gas flow is set to an inertial change with a time constant of 1.2 s. The fuel margin, burner temperature, and NOx emissions of the SOFC system under different power switching strategies are shown in Fig. 7.

Figure 7 shows that although the influence of gas transmission delay is eliminated in the simulation, the step switching strategy experiences fuel starvation during the transition from half load to full load, while the linearity and multi-step switching strategies also experience fuel starvation during the transition from full load to half load. Meanwhile, in addition to the switching strategy based on the change of gas flow designed in this paper, the burner temperature of other strategies will exceed the temperature limit even if there is no fuel starvation.

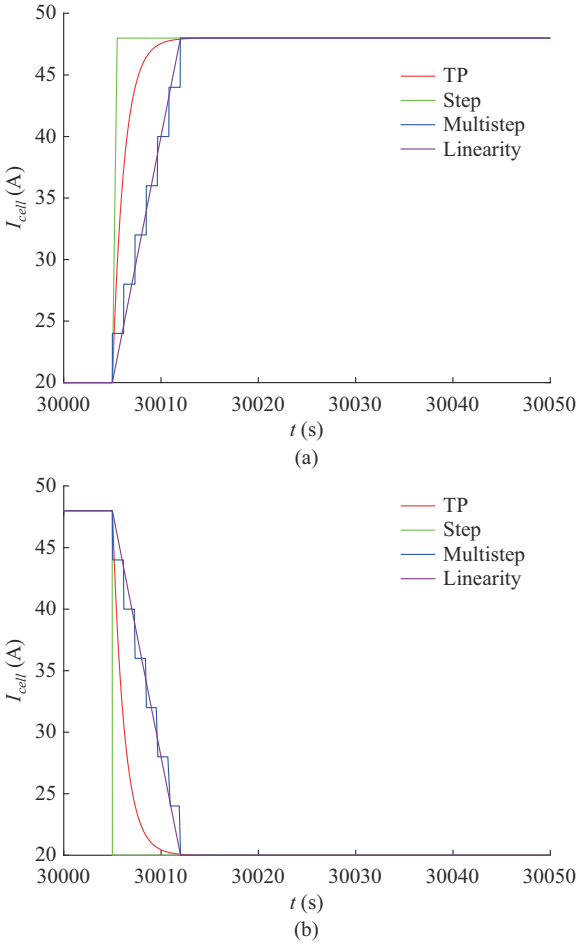

Fig. 6. Stack current for four different switching strategies. (a) I_{cell} from half load to full load. (b) I_{cell} from full load to half load.

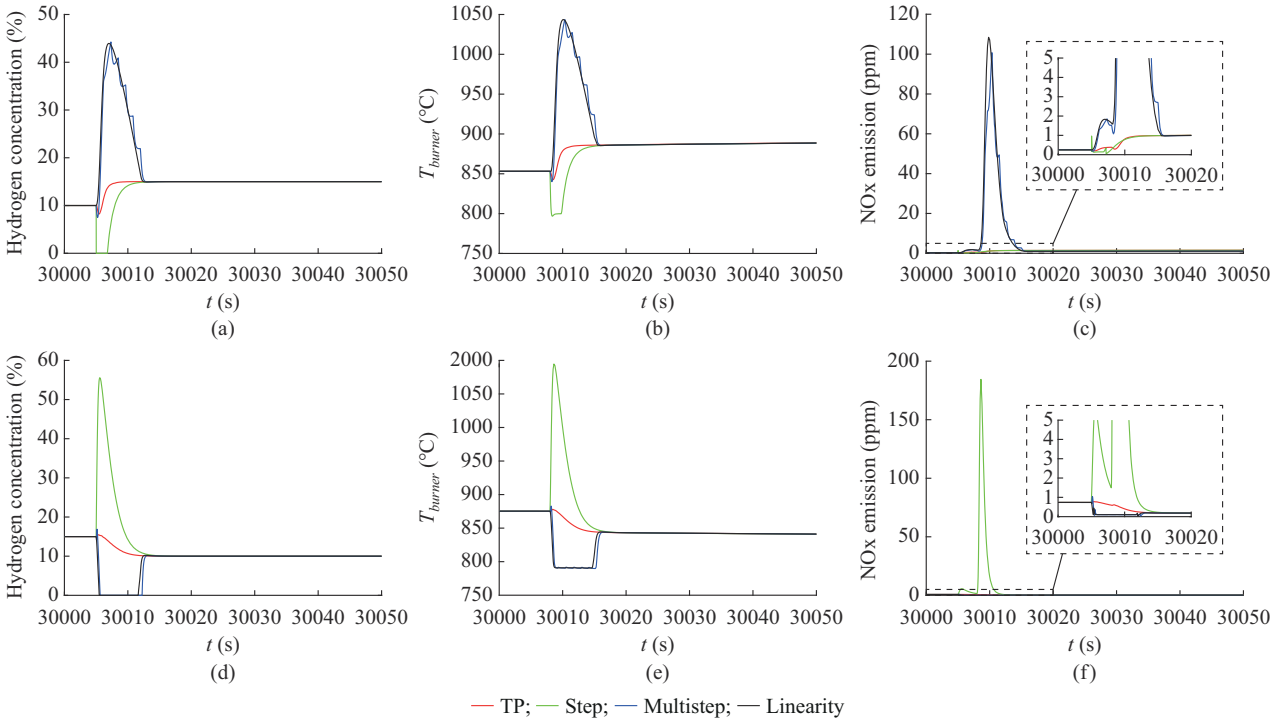

Fig. 7. Performance of different power switching strategies. (a) Hydrogen concentration from half load to full load. (b) T_{burner} from half load to full load. (c) NOx emission from half load to full load. (d) Hydrogen concentration from full load to half load. (e) T_{burner} from full load to half load. (f) NOx emission from full load to half load.

Furthermore, due to the extremely high burner temperature, the NOx emissions of other strategies are also much higher than the TP. Through comparison, it can be observed that the power switching strategy designed in this paper is far superior to other power switching strategies.

V. Improved Power Switching Strategy with SMC

In the previous section, a power switching strategy based on TP is designed. Subsequent comparative verification also proves the superiority of this power switching strategy. However, the power switching strategy based on TP also has problems: it is necessary to know the exact changing trajectory of gas flow and the exact gas transmission delay time, which is impossible to achieve in the actual process. When the trajectory of gas flow and the gas transmission delay time change, the actual control effect will be affected greatly. In order to solve this problem, this paper introduces the SMC based on the power switching strategy mentioned above, ensuring the system control performance in the case of inaccurate gas flow trajectory and gas transmission delay time.

A. Power Switching with SMC

In this subsection, the changing trajectory of hydrogen concentration at the stack outlet is defined as the predicted trajectory of hydrogen. The control objective of this paper is to ensure that the actual hydrogen concentration at the stack outlet tends towards the predicted trajectory of hydrogen when the gas flow and gas transmission delay time change. The specific control schematic is shown in Fig. 8.

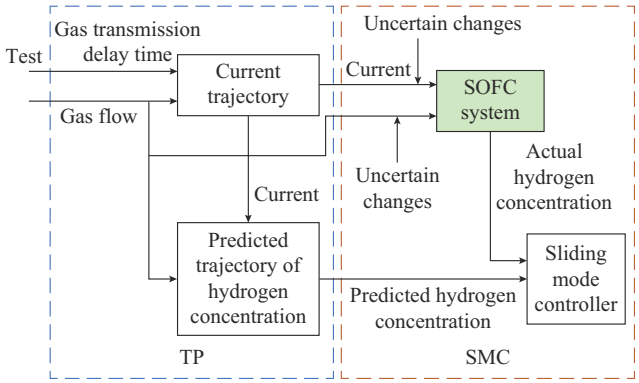

Fig. 8. Schematic diagram of power switching control for SOFC system.

1) System Control Model

When the SOFC system is in operation, the SOFC stack satisfies the pneumatic balance. According to the pneumatic balance, the following equation holds:

$$n_{fuel}\dot{\varphi}_{H_2,stack}=N_{fuel,in}\varphi_{H_2,in}-N_{fuel,out}\varphi_{H_2,out}-\frac{I}{2F} \tag{13}$$

where n_{fuel} is the mole number; $\varphi_{H_2,j}, j\in\{in,out\}$ is the gas molar fraction of gas i at position j; $\varphi_{H_2,stack}$ is the average gas molar fraction inside the stack, $\varphi_{H_2,stack}=(\varphi_{H_2,in}+\varphi_{H_2,out})/2$; $N_{fuel,j}, j\in\{in,out\}$ is the molar flow; I is the current of stack; and F is the Faraday constant (96485.33 C/mol).

For the SOFC stack, the inlet gas concentration generally does not change. At the same time, according to the reaction mechanism, $N_{fuel,out}=N_{fuel,in}$. Thus, the above equation can be written as:

$$\frac{n_{fuel}\dot{\varphi}_{H_2,out}}{2}=N_{fuel,in}\varphi_{H_2,in}-N_{fuel,in}\varphi_{H_2,out}-\frac{I}{2F} \tag{14}$$

Under planned and actual conditions, the SOFC stack meets the following equation:

$$\begin{cases}\dfrac{n_{fuel}\dot{\varphi}_{H_2,out,tr}}{2}=N_{fuel,in,tr}\varphi_{H_2,in}-N_{fuel,in,tr}\varphi_{H_2,out,tr}-\dfrac{I_{tr}}{2F}\\ \dfrac{n_{fuel}\dot{\varphi}_{H_2,out,re}}{2}=N_{fuel,in,re}\varphi_{H_2,in}-N_{fuel,in,re}\varphi_{H_2,out,re}-\dfrac{I_{re}}{2F}\end{cases} \tag{15}$$

where subscript *tr* is the planned situation; and subscript *re* is the actual situation.

Let $I_{re}=I_{tr}+\Delta I$ and $e=\varphi_{H_2,out,re}-\varphi_{H_2,out,tr}$. Then:

$$\dot{e}=-\frac{2N_{fuel,in,re}}{n_{fuel}}e-\frac{\Delta I}{n_{fuel}F}+\frac{2(N_{fuel,in,re}-N_{fuel,in,tr})(\varphi_{H_2,in}-\varphi_{H_2,out,tr})}{n_{fuel}} \tag{16}$$

2) Design of SMC

SMC is a well-known nonlinear control method that can be designed through a variable structure control law to first reach the desired manifold and then move along the sliding manifold to reach the equilibrium point [40], [41]. Due to its fast dynamic response, good transient performance, insensitivity to matching uncertainties, robustness to external disturbances, ease of implementation, and finite time convergence, SMC has been shown to be a suitable and effective method for various nonlinear control problems [42]-[45]. Thus, SMC is selected in this paper to control the changing trajectory of hydrogen concentration at the stack outlet.

The design of a sliding mode controller consists of two parts: firstly, it can reach the sliding mode surface $s=0$ in finite time from any position in the state space; secondly, it can converge to the origin (equilibrium point) on the sliding mode surface. The following will provide a detailed introduction to the design of the sliding mode controller in this paper.

According to (16), the dynamical system model can be rewritten as:

$$\begin{cases}\dot{x}=Ax+Bu+C\\ x=e\\ u=\Delta I\\ A=-\dfrac{2N_{fuel,in,re}}{n_{fuel}}\\ B=-\dfrac{1}{n_{fuel}F}\\ C=\dfrac{2(N_{fuel,in,re}-N_{fuel,in,tr})(\varphi_{H_2,in}-\varphi_{H_2,out,tr})}{n_{fuel}}\end{cases} \tag{17}$$

Let $\bar{A}=2N_{fuel,\max}/n_{fuel}$, and $N_{fuel,\max}$ is the maximum fuel flow. For (17), the following equation holds, as shown in Supplementary Material A.

$$|Ax+C|<\bar{A} \tag{18}$$

For the dynamic system in this paper, the following sliding surface is constructed:

$$s = x \tag{19}$$

To ensure that s converges to 0, it is necessary to design the control equation u. According to the second method of Lyapunov stability determination, if there exists a continuous function V that satisfies the following conditions, the system will be stable at equilibrium point $s=0$.

$$\begin{cases} V(0)=0 & \text{condition 1} \\ V(s)>0 & \text{condition 2} \\ \dot{V}(s)<0 & \text{condition 3} \end{cases} \tag{20}$$

Choose a Lyapunov function as:

$$V = \frac{1}{2}s^2 \tag{21}$$

The above equation clearly satisfies conditions (1) and (2). For condition (3), the design control equation $u=(-ks-\bar{A}\cdot\mathrm{sgn}(s))/B=\eta s+\rho\cdot\mathrm{sgn}(s)$, where $k>0$; $\mathrm{sgn}(s)$ is the step function; $\eta=-k/B$ and $\rho=-\bar{A}/B$. Then, we can obtain:

$$\begin{aligned} \dot{V}(s)=s\dot{s}=s(Ax+Bu+C)=s(Ax+C)-s(ks+\bar{A}\cdot\mathrm{sgn}(s))\le \\ -ks^2+|s|(Ax+C)-|s|\bar{A}<-ks^2 \end{aligned} \tag{22}$$

It is obvious that the above equation satisfies condition (3). Thus, the system can be stable at equilibrium point $s=0$.

Due to $|s|=|x|\le 1$, (22) can be written as:

$$\dot{V}(s)<-k|s| \tag{23}$$

It is clear that the system state will reach the sliding mode surface $s=0$ within the finite time t_r, which satisfies:

$$t_r \le \frac{|s(0)|}{k} \tag{24}$$

In summary, the sliding mode controller ($u=\eta s+\rho\cdot\mathrm{sgn}(s)$) designed in this paper can ensure that the system state reaches the sliding mode surface $s=0$ within t_r.

Although the sliding mode controller designed above can ensure that the system state tends to the sliding mode surface within a finite time, it also has two problems in practical use: ① high-frequency traversal caused by excessive controller output; ② difficulty in strictly sliding along the sliding mode towards the equilibrium point when the state trajectory reaches the sliding mode surface. In fact, it will move back and forth on both sides of the sliding surface to approach the equilibrium point. The controller will be improved to address these two problems as follows.

For the first problem, it can be solved by reducing the output of the controller. For the second problem, it can be solved by changing the sliding model surface to the sliding model strip. Based on these two ideas, the improved controller is designed as:

$$u = \begin{cases} \eta s + \dfrac{\rho^2 s}{\rho|s|+\varepsilon} & |s|>0.005, \varepsilon>0 \\ \eta s + 0 & |s|\le 0.005, \varepsilon>0 \end{cases} \tag{25}$$

After verification, the above controller can make the system to be globally uniformly ultimately bounded, and the output tracking error converges to a neighborhood of zero, as shown in Supplementary Material B. We define u_f as the output of controller before improvement, and u_d as the output of the improved controller. Firstly, the issue of sliding mode strip is not considered. When $s=0$, $u_f=u_d=0$; when $s\neq 0$, $u_d=\eta s+\dfrac{\rho^2 s}{\rho|s|+\varepsilon}<\eta s+\rho\dfrac{s}{|s|}, \varepsilon>0$. Obviously, $u_d<u_f$. Therefore, the output of the improved controller is lower than that of the pre-improved controller. Moreover, by changing the sliding mode surface to the sliding mode strip, the chattering during the use of SMC can be effectively reduced.

B. Comparison and Results of Control Performance

In the previous section, the paper designs a sliding mode controller to address the impact of uncertainty in gas flow and gas transmission delay time on actual control performance. To verify the effectiveness of the controller, a comparison will be made between these two different power switching strategies, namely the power switching strategy based on TP and the power switching strategy based on TP-SMC.

Similar to Section IV, assuming that the gas flow is an inertial change with $T=1.2$ s and the gas transmission delay time is 5 s. Then, the trajectory of the stack current and the trajectory of the hydrogen concentration at the stack outlet can be determined (defined as reference trajectory in the following text). Finally, the control effects of different control strategies by changing the gas flow and the gas transmission delay time are compared. To describe the relationship between the reference current switching point and the actual current switching point, we define T_f as the shift time. In addition, through analysis and simulation, it can be known that the burner temperature will only exceed the temperature limit when the hydrogen concentration at the stack outlet exceeds a certain value (approximately 30%). Therefore, this subsection only analyzes the hydrogen concentration at the stack outlet.

Firstly, we change the gas flow. Here, the time constants of the gas flow change process are set to be 0.5 s, 1 s, 1.5 s, and 2 s, respectively. The stack current I_{cell}, hydrogen concentration at the stack outlet, and NOx emissions of the SOFC system under different time constants are shown in Fig. 9.

From Fig. 9, it can be observed that when the gas flow changes, under the control of the TP, the stack current still changes along the planned current trajectory, causing the hydrogen concentration at the stack outlet to deviate from the predetermined trajectory. As the gas flow changes more, the deviation of hydrogen concentration will also increase, and eventually even fuel starvation and temperature exceeding limit will occur. On the contrary, under the control of the TP-SMC, the stack current will shift on the original current trajectory to offset changes in gas flow, and finally control the hydrogen concentration near the predicted trajectory of hydrogen. Although there are deviations in hydrogen concentration under the TP-SMC, the deviation is much smaller than that under the TP control and the hydrogen concentration is within an acceptable range ([5%, 25%]). In addition, under the control of the TP, the temperature will increase with the increase of fuel margin, leading to an increase in NOx emissions in the burner.

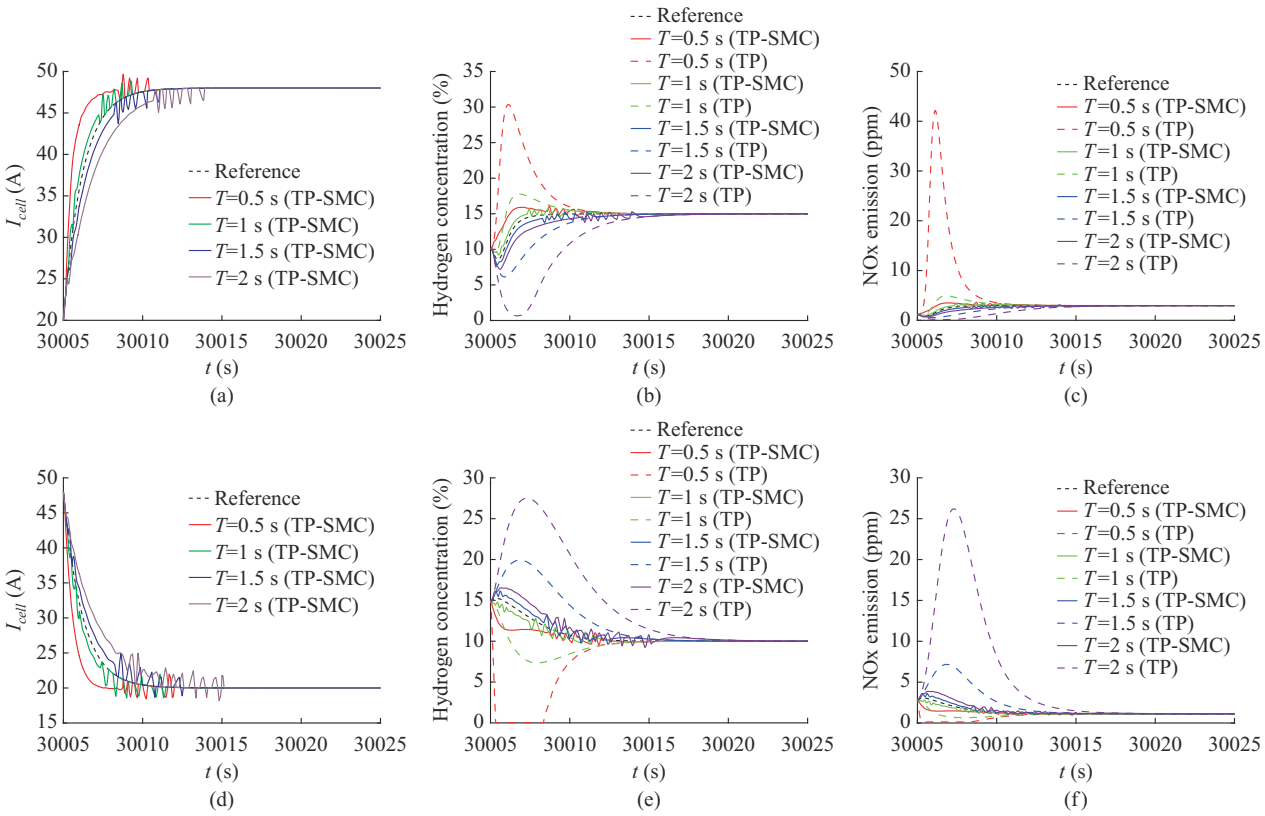

Fig. 9. Control performance comparison under different time constants. (a) I_{cell} from half load to full load. (b) Hydrogen concentration from half load to full load. (c) NOx emission from half load to full load. (d) I_{cell} from full load to half load. (e) Hydrogen concentration from full load to half load. (f) NOx emission from full load to half load.

Although the NOx emissions in the figure are still not very large, the burner temperature will also increase as the gas flow changes more, ultimately leading to a continued increase in NOx emissions. Correspondingly, under the control of the TP-SMC, the NOx emission is at the level of normal operation of the SOFC system. Obviously, compared with the TP, the TP-SMC has better control effect.

Secondly, we change the gas transmission delay time. Here, T_f is set to be −2 s, −1 s, 1 s, and 2 s, respectively. The stack current, hydrogen concentration at the stack outlet, and NOx emissions of SOFC system under different shift time are shown in Fig. 10.

Figure 10 shows that when the gas transmission delay time changes, under the control of the TP, the stack current will shift laterally by a value on the original current trajectory based on the amount of time change. Finally, under the T_f set in the paper, all SOFC systems will experience fuel starvation or temperature exceeding limit. This indicates that the shift of the current switching point has a significant impact on the actual control. Relatively, under the control of the TP-SMC, although the trajectory of hydrogen concentration at the stack outlet also has a certain deviation, it is within the normal range, and all SOFC systems will not experience fuel starvation and temperature exceeding limit. In addition, in terms of NOx emissions, the NOx emissions under the TP control increase sharply after the current switching point shifts beyond a certain range, which is clearly to be avoided during the actual power switching process. In contrast, the NOx emissions under the control of the TP-SMC are all very low and within the normal and acceptable range (< 50 ppm). It is worth noting that the shift of 2 s is already significant and the measurement error generally does not exceed this range in practice. In summary, the power switching strategy based on TP-SMC designed in this paper is effective and can solve the problems in the TP.

VI. Conclusion

In this paper, a power switching strategy based on the TP -SMC is designed. Through the test, the change law of actual gas flow is determined, and the possible safety issues and NOx emission characteristics in the actual power switching process are determined through simulation. In addition, the design elements of the power switching strategy are proposed. Due to the delay in gas transmission, when designing the power switching strategy, the gas transmission delay time is first determined through test to obtain the current switching point. Then, the TP is proposed based on the delay of gas transmission and the change of gas flow. In order to verify the superiority of the TP proposed in this paper, it is also compared with other power switching strategies. The results also prove that the power switching strategy designed in this paper has better performance.

Although the TP has good control effects, it also has flaws that make it problematic in practical application. Therefore, this paper introduces SMC based on TP.

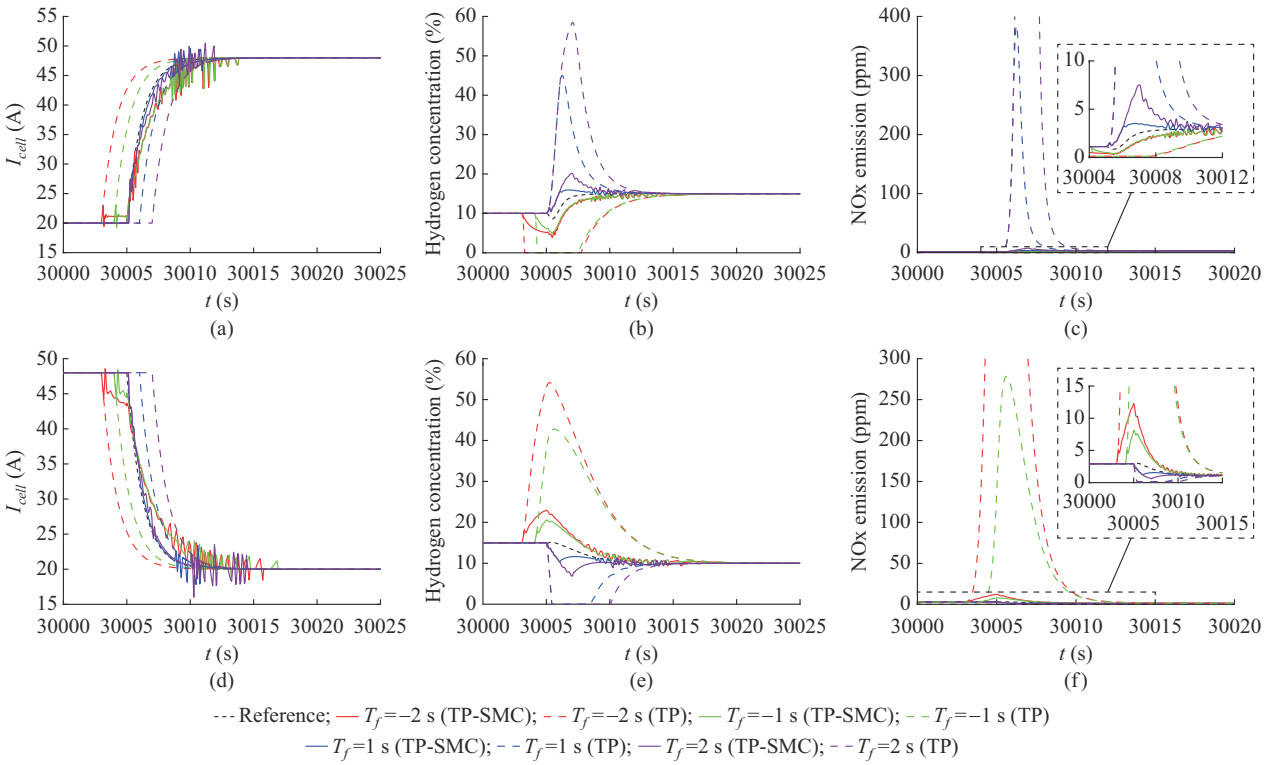

Fig. 10. Control performance comparison under different shift time. (a) I_{cell} from half load to full load. (b) Hydrogen concentration from half load to full load. (c) NOx emission from half load to full load. (d) I_{cell} from full load to half load. (e) Hydrogen concentration from full load to half load. (f) NOx emission from full load to half load.

The final simulation results also prove that the TP-SMC can effectively suppress the impact of uncertainty in gas flow and gas transmission delay time. Compared with TP, TP-SMC can ensure that under uncertain conditions, the SOFC system does not experience fuel starvation and temperature exceeding limit during power switching. At the same time, the NOx emissions during the power switching process are also within the normal and acceptable range.

The power switching strategy designed in this paper can effectively avoid the safety issues of fuel starvation and temperature exceeding limit in the SOFC systems during power switching. Fuel starvation may lead to stack oxidation, and temperature exceeding limit may damage the burner. Therefore, the research in this paper can improve the safety performance and service life of the system. In addition, the power switching strategy designed in this paper can also ensure that the SOFC system generates very low pollutants during the power switching process, making it more environmentally friendly.

REFERENCES

[1] K. Lee, S. Kang, and K.-Y. Ahn, "Development of a highly efficient solid oxide fuel cell system," *Applied Energy*, vol. 205, pp. 822-833, Nov. 2017.

[2] V. Sinha and S. Mondal, "Recent development on performance modelling and fault diagnosis of fuel cell systems," *International Journal of Dynamics & Control*, vol. 6, no. 2, pp. 511-528, Apr. 2018.

[3] M. Singh, D. Zappa, and E. Comini, "Solid oxide fuel cell: Decade of progress, future perspectives and challenges," *International Journal of Hydrogen Energy*, vol. 46, no. 54, pp. 27643-27674, Aug. 2021.

[4] X. Zhang, S. Chan, G. Li *et al*., "A review of integration strategies for solid oxide fuel cells," *Journal of Power Sources*, vol. 195, no. 3, pp. 685-702, Mar. 2010.

[5] J. Peng, J. Huang, X. Wu *et al*., "Solid oxide fuel cell (SOFC) performance evaluation, fault diagnosis and health control: a review," *Journal of Power Sources*, vol. 505, p. 230058, Sept. 2021.

[6] R. Barrera, S. de Biase, S. Ginocchio *et al*., "Performance and life time test on a 5 kW SOFC system for distributed cogeneration," *International Journal of Hydrogen Energy*, vol. 33, no. 12, pp. 3193-3196, Jun. 2008.

[7] Y. Kawabata, Y. Tachikawa, S. Taniguchi *et al*., "New applications of SOFC-MGT hybrid power generation system for low-carbon society," *ECS Transactions*, vol. 78, no. 1, p. 197, May 2017.

[8] M. Suzuki, S. Inoue, and T. Shigehisa, "Field test result of residential SOFC CHP system over 10 years, 89000 hours," *ECS Transactions*, vol. 103, no. 1, p. 25, Jul. 2021.

[9] H. Tu and U. Stimming, "Advances, aging mechanisms and lifetime in solid-oxide fuel cells," *Journal of Power Sources*, vol. 127, no. 1, pp. 284-293, Mar. 2004.

[10] F. Mueller, F. Jabbari, and J. Brouwer, "On the intrinsic transient capability and limitations of solid oxide fuel cell systems," *Journal of Power Sources*, vol. 187, no. 2, pp. 452-460, Feb. 2009.

[11] C. Lin, T. Chen, Y. Chyou *et al*., "Thermal stress analysis of a planar SOFC stack," *Journal of Power Sources*, vol. 164, no. 1, pp. 238-251, Jan. 2007.

[12] J. Jiang, R. Zhou, H. Xu, "Optimal sizing, operation strategy and case study of a grid-connected solid oxide fuel cell microgrid," *Applied Energy*, vol. 307, p. 118214, Feb. 2022.

[13] H. Xi, "Dynamic modeling and control of planar SOFC power systems," Ph.D dissertation, Department of Naval Architecture and Marine Engineering, University of Michigan, Ann Arbor, United States, 2007.

[14] H. Cao, X. Li, Z. Deng *et al*., "Thermal management oriented steady state analysis and optimization of a kW scale solid oxide fuel cell stand-alone system for maximum system efficiency," *International Journal of Hydrogen Energy*, vol. 38, no. 28, pp. 12404-12417, Sept. 2013.

[15] H. Cheng, S. Jing, Y. Xu *et al*., "Control-oriented modeling analysis and optimization of planar solid oxide fuel cell system," *International Journal of Hydrogen Energy*, vol. 41, no. 47, pp. 22285-22304, Dec. 2016.

[16] X. Wu and D. Gao, "Optimal robust control strategy of a solid oxide fuel cell system," *Journal of Power Sources*, vol. 374, pp. 225-236, Jan. 2018.
[17] A. Omer, I. Rahimipetroudi, K. Rashid *et al*., "Design and performance optimization of a direct ammonia planar solid oxide fuel cell for high electrical efficiency," *Journal of Power Sources*, vol. 573, p. 233135, Jul. 2023.
[18] L. Zhang, X. Li, J. Jiang *et al*., "Dynamic modeling and analysis of a 5-kW solid oxide fuel cell system from the perspectives of cooperative control of thermal safety and high efficiency," *International Journal of Hydrogen Energy*, vol. 40, no. 1, pp. 456-476, Jan. 2015.
[19] L. Zhang, J. Jiang, H. Cheng *et al*., "Control strategy for power management, efficiency-optimization and operating-safety of a 5-kW solid oxide fuel cell system," *Electrochimica Acta*, vol. 177, pp. 237-249, Sept. 2015.
[20] J. Jiang, T. Shen, Z. Deng *et al*., "High efficiency thermoelectric cooperative control of a stand-alone solid oxide fuel cell system with an air bypass valve," *Energy*, vol. 152, pp. 13-26, Feb. 2018.
[21] R. Gaynor, F. Mueller, F. Jabbari *et al*., "On control concepts to prevent fuel starvation in solid oxide fuel cells," *Journal of Power Sources*, vol. 180, no. 1, pp. 330-342, May 2008.
[22] F. Mueller, F. Jabbari, R. Gaynor *et al*., "Novel solid oxide fuel cell system controller for rapid load following," *Journal of Power Sources*, vol. 172, no. 1, pp. 308-323, Oct. 2007.
[23] T. Zhang and G. Feng, "Rapid load following of an SOFC power system via stable fuzzy predictive tracking controller," *IEEE Transactions on Fuzzy Systems*, vol. 17, no. 2, pp. 357-371, Apr. 2009.
[24] M. Nayeripour and M. Hoseintabar, "A new control strategy of solid oxide fuel cell based on coordination between hydrogen fuel flow rate and utilization factor," *Renewable and Sustainable Energy Reviews*, vol. 27, pp. 505-514, Nov. 2013.
[25] P. Gupta, V. Pahwa, and Y. P. Verma, "Load tracking enhancement of a grid connected SOFC system using an advanced controller in real time," in *Proceedings of 2020 First IEEE International Conference on Measurement, Instrumentation, Control and Automation (ICMICA)*, Kurukshetra, India, Jun, 2020, pp. 1-6.
[26] Z. Wang, G. Liu, and X. Liu, "Inconsistency analysis and power allocation of the stack in multi-stack solid oxide fuel cell system," *Journal of Power Sources*, vol. 598, p. 234163, Apr. 2024.
[27] H. Cao, Z. Deng, X. Li *et al*., "Dynamic modeling of electrical characteristics of solid oxide fuel cells using fractional derivatives," *International Journal of Hydrogen Energy*, vol. 35, no. 4, pp. 1749-1758, Feb. 2010.
[28] M. Ni, M. K. Leung, and D. Y. Leung, "Parametric study of solid oxide fuel cell performance," *Energy Conversion and Management*, vol. 48, no. 5, pp. 1525-1535, May 2007.
[29] W. Gong, Z. Cai, J. Yang *et al*., "Parameter identification of an SOFC model with an efficient, adaptive differential evolution algorithm," *International Journal of Hydrogen Energy*, vol. 39, no. 10, pp. 5083-5096, Mar. 2014.
[30] H. Xi and J. Sun, "Dynamic analysis of planar solid oxide fuel cell models with different assumptions of temperature layers," *Journal of Fuel Cell Science and Technology*, vol. 6, no. 1, pp.1-12, Feb. 2008.
[31] A. M. Murshed, B. Huang, and K. Nandakumar, "Control relevant modeling of planer solid oxide fuel cell system," *Journal of Power Sources*, vol. 163, no. 2, pp. 830-845, Jan. 2007.
[32] N. Lu, Q. Li, X. Sun *et al*., "The modeling of a standalone solid-oxide fuel cell auxiliary power unit," *Journal of Power Sources*, vol. 161, no. 2, pp. 938-948, Oct. 2006.
[33] L. S. Caretto, "Mathematical modeling of pollutant formation," in *Energy and Combustion Science*, Cambridge: Pergamon, 1979, pp. 49-73.
[34] S. Hill and L. D. Smoot, "Modeling of nitrogen oxides formation and destruction in combustion systems," *Progress in Energy and Combustion Science*, vol. 26, no. 4, pp. 417-458, Aug. 2000.
[35] A. A. Konnov, G. Colson, and J. de Ruyck, "NO formation rates for hydrogen combustion in stirred reactors," *Fuel*, vol. 80, no. 1, pp. 49-65, Jan. 2001.
[36] M. Abian, M. U. Alzueta, and P. Glarborg, "Formation of NO from N_2/O_2 mixtures in a flow reactor: toward an accurate prediction of thermal NO," *International Journal of Chemical Kinetics*, vol. 47, no. 8, pp. 518-532, Sept. 2015.
[37] D. L. Baulch, C. J. Cobos, R. A. Cox *et al*., "Summary table of evaluated kinetic data for combustion modeling: supplement 1," *Combustion and Flame*, vol. 98, no. 1, pp. 59-79, Jul. 1994.
[38] A. A. Westenberg, "Kinetics of NO and CO in lean, premixed hydrocarbon-air flames," *Combustion Science and Technology*, vol. 4, no. 1, pp. 59-64, Sept. 1971.
[39] P. J. Coelho and M. G. Carvalho, "Mathematical modelling of NO formation in a power station boiler," *Combustion Science and Technology*, vol. 108, no. 4, pp. 363-382, Jan. 1995.
[40] S. Liu, Y. Sang, and J. F. Whidborne, "Adaptive sliding-mode-backstepping trajectory tracking control of underactuated airships," *Aerospace Science and Technology*, vol. 97, p. 105610, Feb. 2020.
[41] S. Liu, J. F. Whidborne, W. Lyv *et al*., "Observer based incremental backstepping terminal sliding-mode control with learning rate for a multi-vectored propeller airship," *Aerospace Science and Technology*, vol. 140, p. 108490, Sept. 2023.
[42] Y. Mousavi, G. Bevan, I. B. Kucukdemiral *et al*., "Sliding mode control of wind energy conversion systems: trends and applications," *Renewable and Sustainable Energy Reviews*, vol. 167, p. 112734, Oct. 2022.
[43] A. D. Falehi and H. Torkaman, "Promoted supercapacitor control scheme based on robust fractional-order super-twisting sliding mode control for dynamic voltage restorer to enhance FRT and PQ capabilities of DFIG-based wind turbine," *Journal of Energy Storage*, vol. 42, p. 102983, Oct. 2021.
[44] A. D. Falehi, "An optimal second-order sliding mode based inter-area oscillation suppressor using chaotic whale optimization algorithm for doubly fed induction generator," *International Journal of Numerical Modelling: Electronic Networks, Devices and Fields*, vol. 35, no. 2, p. 2963, Apr. 2022.
[45] A. D. Falehi, "Optimal robust disturbance observer based sliding mode controller using multi-objective grasshopper optimization algorithm to enhance power system stability," *Journal of Ambient Intelligence and Humanized Computing*, vol. 11, no. 11, pp. 5045-5063, Nov. 2020.

Zhen Wang received the B.S. degree in mechanical design manufacture and automation and the M.S. degree in mechanical engineering from the Central South University, Changsha, China, in 2017 and 2020, respectively. He is currently pursuing the Ph.D. degree with the Huazhong University of Science and Technology, Wuhan, China. His research interests include solid-oxide electrochemical sensor, electrochemical kinetics in solids, solid oxide fuel cell system modeling, and system control and performance optimization.

Guoqiang Liu received the M.S. degree from Dalian Maritime University, Dalian, China, in 2020. He is currently pursuing the Ph.D. degree with the School of Artificial Intelligence and Automation, Huazhong University of Science and Technology, Wuhan, China. His research interests include renewable energy system integration and optimization, and hydrogen energy conversion and management technologies.

Xingbo Liu holds a postgraduate degree in geographic information science from Wuhan University, Wuhan, China. He is a Director of the Information Technology department at the Hubei Huazhong Electric Power Technology Development Co., Ltd., Wuhan, China. His research interests include surveying and mapping, digital infrastructure platform construction, digital system architecture design, and new power system.

Jie Wang received the M.S degree in control theory and control engineering from Huazhong University of Science and Technology, Wuhan, China, in 2017. He is currently pursuing the Ph.D. degree with the Huazhong University of Science and Technology. His research interests include measurement and control of vehicle nitrogen oxygen sensor, measurement and integration of solid oxide cell system.

Zhiyang Jin is pursuing the bachelor degree at Huazhong University of Science and Technology, Wuhan, China. His research interests include process control and new power system.

Xiaowei Fu received the Ph.D. degree in control science and engineering from the Huazhong University of Science and Technology, Wuhan, China, in 2010. She is currently a Professor with the School of Computer Science and Technology, Wuhan University of Science and Technology, Wuhan, China. Her research interests include computer vision, image processing, machine learning, and intelligent control.

Zhuo Wang received the M.S. and Ph.D. degrees in control theory and control engineering from the Huazhong University of Science and Technology, Wuhan, China, in 2003 and 2008, respectively. He is currently a Lecturer with the School of Artificial Intelligence and Automation, Huazhong University of Science and Technology. His research interests include process con-

trol and smart grid.

Bing Jin received the bachelor degree from Huazhong University of Science and Technology, Wuhan, China, 2007. She works with Hubei Huazhong Electric Power Technology Development Co., Ltd., Wuhan, China, as a Deputy Director in Research and Development Department. Her research interests include safety management and risk supervision in platform construction, digital infrastructure platform, digital system architecture, product design, and new power system.

Zhonghua Deng received the Ph.D. degree in control theory and control engineering from the Huazhong University of Science and Technology, Wuhan, China, in 1994. He is a Professor of Huazhong University of Science and Technology. His research interests include intelligent control, digital control of electric drive system, advance control strategy, and machine learning.

Xi Li received the Ph.D. degree from Shanghai Jiao Tong University, Shanghai, China, in 2006. From 2011 to 2012, he was a Visiting Scholar with the Naval Architecture and Marine Engineering Department, University of Michigan, Ann Arbor, USA. He has been with the Huazhong University of Science and Technology, Wuhan, China, since 2006, where he is currently a Professor with the School of Artificial Intelligence and Automation. His research interests include intelligent control and model predictive control of renewable energy systems.